



Influence of structural parameters on the properties of fibred-foamed concrete

Y. H. Mugahed Amran^{1,2}

Received: 31 August 2019 / Accepted: 7 January 2020 / Published online: 5 February 2020
© Springer Nature Switzerland AG 2020

Abstract

The demand for novel technology for manufacturing lightweight concrete has increased in the global construction industry. Therefore, studies that explore alternative lightweight concrete systems for structural applications are urgently needed. The objective of this study is to develop structural fibred-foamed concrete (SFFC) by the addition of polypropylene (PP) fibre, fly ash (FA), and silica fume (SF). Foamed concrete (FC) was obtained by replacing sand with FA. The properties of the FC were enhanced with PP fibre and fine SF. SFFC with dissimilar densities of FC (1000, 1300, 1600, and 1900 kg/m³) is essential for examining compressive, flexural, and splitting tensile strengths, drying shrinkage, and creep. The FC with a density of 1000–1900 kg/m³ and compressive and splitting tensile strengths of 10–70 MPa and 1.1–4.81 MPa, respectively, have been made by the addition of PP fibre and fine SF. Fine SF and PP fibre considerably improved the hardened strength of the FC. Additionally, the inclusion of PP fibre significantly enhanced the tensile strength and increased the creep resistance and drying shrinkage. Therefore, SFFC can be used as a substitute lightweight concrete material for the production of structural concrete applications in the construction industries today.

Keywords Creep, shrinkage · Foam agent · Lightweight concrete · Foamed concrete (FC) · PP fibre · Fibre-reinforced materials · High-strength concrete · Compressive, flexural, and splitting tensile strengths

Introduction

Foamed concrete (FC), also known as cellular concrete, receives considerable attention from builders worldwide [1, 2]. The rapidly growing demand for energy-saving and environment-friendly construction technology is driving this shift in focus [3, 4]. Neat cement with fine sand is used in the fabrication of lightweight FC with discrete, uniformly distributed, micro- or macroscopic air cells [3, 5–9]. FC provides unique advantages such as thermal and acoustic insulation and resistance to fire and termite attacks, lowers costs in construction, and produces low self-weight and eco-friendly structures [10–16]. There are two common methods used for producing FC, called method A and method B. Method A

involves mixing foaming agents into slurry made from water and cement [17]. When the concrete strengthens, the foams degenerate, and air bubbles of uniform size remain. Meanwhile, method B is practically applied in the production of autoclaved aerated concrete (AAC), which is a mixture of cement, water, sand, and lime with an amplification agent, generally aluminium dust, decanted into a mould [8, 18]. The concrete mixture expands about 500% its actual size due to the microscopic hydrogen foams produced from the interaction between cement and aluminium dust. When the hydrogen bubbles evaporate, the AAC is censored into a specified volume and treated at steam condition in an autoclave or a pressure chamber [17, 19]. The concept of AAC was developed approximately one century ago, and this technique is gaining traction in construction industries [20]. It has been applied effectively in more than 40 countries. No restriction in size or casting of AAC is specified because it is controlled by the requirements of factory autoclaving. However, all of these requirements can be fulfilled by FC, which can be produced by method A [9, 17, 18]. Concrete with a density of around 400–1800 kg/m³ and the ability to flow and self-compact can be produced through method A [1, 3].

✉ Y. H. Mugahed Amran
m.amran@psau.edu.sa; mugahed_amran@hotmail.com

¹ Department of Civil Engineering, College of Engineering, Prince Sattam Bin Abdulaziz University, Alkharj 11942, Saudi Arabia

² Department of Civil Engineering, Faculty of Engineering and IT, Amran University, 9677 Quhal, Amran, Yemen

Generally, FC is designed to achieve a low compressive strength, around 1–10 MPa, and can be applicable in filling voids and restoring trenches, but it cannot be used in the construction of any structural member [1, 11–13, 16, 21]. To achieve the desired strength of at least 25 MPa, engineers and designers practice different innovative solutions that are economically and environmentally admissible [1, 21, 22]. A small water-to-binder (w/b) ratio and the inclusion of silica fume (SF), ultrafine powder of silica, and fly ash (FA) as an alternative to sand are recommended in the production of high-strength FC [7, 10, 23]. A number of studies produced FC with a compressive strength of around 50 MPa by applying special curing conditions and emphasized the relationships between strength, density, and porosity [2, 3, 5, 8, 22, 24, 25]. Several studies have focused on the performance and behaviour of FC, but few addressed the development of high-strength FC [1, 4, 5, 19, 22, 26]. A high-strength, polypropylene- (PP) fibre-reinforced FC was described by Brothers et al. [27]. The present paper attempts to develop structural fibred-foamed concrete (SFFC) with 10–70 MPa compressive strength, 1.2–4.81 MPa splitting tensile strength, and 1000–1900 kg/m³ density. However, there are rare work used fibres to enhance the hardened properties of FC, except focusing on their influences in ordinary concrete performance [28, 29] and for sandy soil [30]. It is also was merely studied on the influence of fibres and foam agent by volume on FC and merely focused on the influential parameter by density, except to some works [19, 35] developed SFFC with the 28-day compressive strength and splitting tensile strengths not even exceeding 50 MPa and 2.5 MPa, respectively. However, FC containing SF as a replacement for cement up to a certain level was studied. The performance properties of SFFC, resistance to creep and shrinkage and thermal conductivity, were studied as a function of the curing period, w/b ratio, foam volume, and PP fibre.

Table 1 Chemical structures of cementing materials, per 1 m³

The chemical compound	Chemical composition (%)		
	Condensed silica fume	Fly ash	Ordinary Portland cement
Aluminium oxide (Al ₂ O ₃)	0.83	24.79	4.24
Silicon dioxide (SiO ₂)	91.9	53.79	21.10
Sodium oxide (Na ₂ O)	–	0.35	0.12
Calcium oxide (CaO)	0.89	8.35	63.45
Magnesium oxide (MgO)	0.23	1.69	1.14
Ferric oxide (Fe ₂ O ₃)	0.54	6.67	4.57
Potassium oxide (K ₂ O)	–	0.103	0.58
Sulphur trioxide (SO ₃)	0.27	0.67	1.69
Loss on ignition	2	0.19	0.72

Experiment details

Proportions of materials and mix

Ordinary Portland cement (OPC), which has a hardened strength of 75.8 MPa, fulfils all the requirements of ASTM Type I cement. Thus, it was used to prepare the specimens for this investigation. The chemical structures of the cement, SF, and FA are provided in Table 1. Dry and un-compacted SF with a SiO₂ content of 91.9% was used in this test. A residue of approximately 1.56% was obtained after sieving the residue through a 45-Am sieve. Class F FA was used in accordance with ASTM C 618 [31]. PP fibre with a 100- μ m diameter and 10-mm length was used (Table 2). Its characteristics are presented in Table 3. A protein-based foam agent with an aerated density of 80 kg/m³ was used after diluting the water with chemical foam in a ratio of 1: 40 (by volume; Tables 4 and 5).

A naphthalene-based superplasticizer was applied in the fabrication of flexible and sufficiently flowable mixtures (Table 5). The dosage of the superplasticizer and the flow of premix paste were low, and the attraction between cement particles was significant. However, the bubbles only adhered along the exterior of the cement particle clusters. Meanwhile, the bubbles might have bonded together and prevented the contact of various clusters formed by the cement particles. Therefore, the bonding between the cement particle clusters weakened. Hence, a cohesive state was observed in the final FC mixture, in which the cementitious particles appeared to be wrapped by the foam. Furthermore, only one

Table 2 PP fibre characteristics, per 1 m³

Length (mm)	Diameter (μ m)	Density (g/cm ³)	Modulus (GPa)	Elongation at break (%)	Tensile strength (MPa)
14.8–15.0	100.0	0.93	8.27	8.03	8.11

Table 3 Fibres characteristics

Property	Type of fibres		
	Polypropylene	Poly-vinyl alcohol	Polypropylene
Denier	1000	1500	15
Fibre length, mm	12	25	12
Specific gravity (S.S.D.)	0.92	1.31	0.94
Modulus of elasticity, GPa	3.46	29	3.48
Tensile strength, GPa	2.69	0.90	2.79
Fibre diameter, μ m	587	398	25

Table 4 Foam agent characteristics

Foam type	AK-350
Colour	Dark brown
PH	6.5–7.5
Density	1.19–0.002
Sediment	Max. 2%
Max. viscosity at 20%	30 Cst
Max. viscosity at 20%	Around 1 to 20

Table 5 Superplasticizer characteristics

Property	Result
Consistency	Liquid
Colour	Dark brown
Density (g/cm ³)	1.13 ± 0.03
Recommended dosage (%)	0.3–2.0
Chlorides content	Nil
PH	4.8
Solids content (%)	30

Table 6 Type of sand used

Property	Southeast Asian sand
Colour	Yellow
Specific gravity (S.S.D.)	2.56
Surface	Smooth
Fineness modulus	1.72
Chloride content (by mass of aggregate):	Not detected
Acid soluble sulphate content (by mass of aggregate)	

type of Middle Eastern sand was used, which had spherical and smooth-surfaced sand particles. The salt content and physical characteristics of the sand are tabulated in Table 6. The sand grading curves are revealed in Fig. 1. The details on the concrete mixture and proportion of ingredients are depicted in Table 7.

Preparation, mixing, fabrication, curing, and testing of SFFC specimens

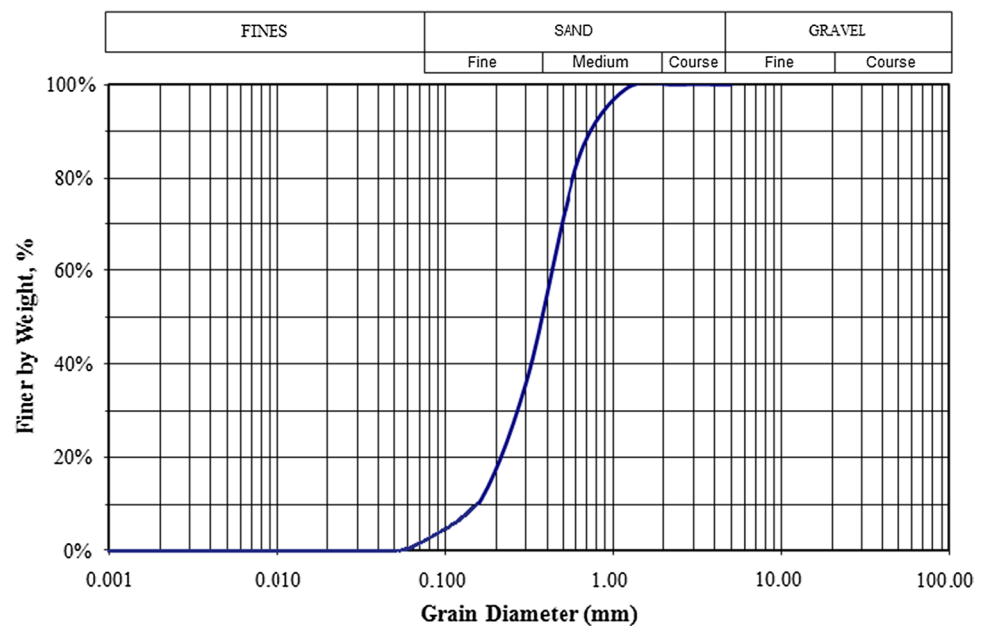
FC was prepared in the workroom by adding the preformed foam to a main mixture and homogenizing the mixture with a paddle mixer. Three different types of FC were produced: Sequence I, which contains FA and cement as the binder; Sequence II, which consists of combining SF, FA, and cement as the binder; and Sequence III, in which only cement was used as the binder in the trial mixes. It was then combined with cement, FA, and SF as the binder. The

proportions are presented in Table 7. The homogenous main mixture was prepared by combining and mixing continuously the binding materials with a specified amount of water. Then, PP fibres were added to this base mix and blended for an additional 3 min. The necessary weight of the foam agent was computed from the volume and density of the foaming included. At that juncture, the foam agent was added to the main mixture. The prepared matrix was then mixed until no noticeable physical mark of the froth can be seen on the surface of matrix, and the froth was consistently dispersed throughout the mix. The effective density of the prepared FC was measured by obtaining its accurate weight and volume. A typical variation of around 50–100 kg/m³ was fixed between the actual and design density of the FC. As shown in Table 7, this variation was within the limits of acceptance.

The ASTM C 469 [32] was used to evaluate the modulus of elasticity of SFFC. The protocol of the test was started after one hour from the time of removing the moulded cylindrical sample from the curing room. The test samples were kept at room temperature as stably as possible during the procedure of the test. In this test, three samples were used to determine the compressive strength before proceeding to the modulus of elasticity test. The strain gauges were fixed in the faces of the test samples as a part of measuring equipment, and then, the samples were positioned on the bearing block of the testing machine. Meanwhile, the test samples were aligned with the centre of force of the spherically placed, higher bearing block and carefully loaded in order to seat the gauges and detect their performance. Subsequently, the load was continuously applied, and the longitudinal strain and applied load were then recorded when the longitudinal strain was almost 50 millionths, and the applied load was equal to 40% of the eventual load of compressive strength.

A set of standardized test samples of variable sizes were chosen with which to investigate selected properties. Cubic samples of 150 mm were fabricated for the studying of concrete compressive strength at a curing time of 3, 7, 14, 28, 56, and 90 days and tensile strength at 28 days. Prism beams of 100 mm × 100 mm × 525 mm were utilized for shrinkage examination at 3, 7, 14, 28, 60, and 90 days. For each mix, twenty-five 100-mm cubical specimens and four prism beams were casted. The samples were hardened for one day after casting and then positioned in a mist room with 95 ± 3% relative humidity (RH) and 22 ± 2 °C temperature conditions. For the testing of shrinkage, the samples were placed for curing in the moulds in a mist room for 23.5 ± 0.5 h. After hardening, the samples were removed from the moulds and shifted to a testing condition (20 ± 3 °C, RH > 60%). The initial values were immediately recorded. Then, the samples were placed in the remedial room again and treated for a specified period. After curing, the samples’ surface water was dehydrated with a moist rag. Then, change in span was recorded for

Fig. 1 Grading curves (% of passing) of the sand



the calculation of the strain of shrinkage in line with the ASTM C 490 [33]. The hardened strength test was conducted in a hydraulic machine of a 2000 kN load capacity and a 5 kN/s loading rate. The tensile strength test was carried out in accordance with ASTM C 496 [32]. The major findings correspond to the average of the data observed from a minimum of three tests on each type of specimen. During this experiment, the deviation of the results was less than 10% of the average value. The actual fresh densities of the developed FC are shown in Fig. 2. In all of the mixtures, the difference between the desired and actual wet density was observed to be within the specified limit of not exceeding 10% of the desired wet density. Practically speaking, a sufficient flow range in a premixed paste is a proof of the effective production of FC. When the value of flow seen was lesser than the limit, the combination of the developed premixed paste and the foam was considered incohesive. The binders seemed to be covered by air bubbles, which collapsed afterwards. However, when the value of flow was greater than the limit, seclusion happened, and the foam bubbles were inclined to collapse. As a finding, the surface of the FC solidified, and the quality of the developed FC was poor because the bubbles did not stabilize within the mortar. Moreover, the hardened FC contained large voids; as a result, the premixed paste possessed a low flow value [34, 35]. The size of the voids relies on the superiority of the premixed paste, if the condition of the foam remains the same before mixing. The most likely reason for the large voids is that small foam bubbles collided and conjoined into larger bubbles and thereby produced larger voids in the hardened FC. The creep test in compression was conducted on Series I, II,

and III specimens in line with the ASTM C 512 standard [36], excluding the possibility that the RH and temperature were varied.

Results and discussion

Influential parameters of compressive strength

Curing time

The development of strength along with the curing time for the FC is shown in Fig. 3. A general increasing trend was observed in the hardened strength of FC with increasing time. The percentage of strength growth was initially prominent but reduced with age (Fig. 4). Nevertheless, after 7 days of curing, the concrete without SF attained approximately 65–80% of its strength at 28 days; meanwhile, the specimens encompassing SF gained approximately 80–95% of the identical 28-day strength. Valuation between the hardened strength developed at 28 and 90 days marked a substantial development in strength with age at the later stage. As observed in FC without SF, the 90-day strength was approximately 75–90% of the conforming 28-day strength. Meanwhile, specimens encompassing SF gained around 80–95% of the equivalent 90-day strength. Therefore, the FC with FA can gain strength over a long period. Similarly, Kearsley and Visagie [37] reported that the strength of 45 MPa can possibly be accomplished by a 56-day-old FC with a 1500 kg/m³ density through the use of unclassified FA, which has 40% of particles and a diameter larger than 45 μm. Another researcher [37] developed an FC with a compressive strength

Table 7 Mix design proportions (constituents) per 1 m³

Series	Mix number	Target density (kg/m ³)	Cement (kg)	Composition of mixture (per m ³)						Fresh density (kg/m ³)		
				Silica fume (kg)	Fly ash (kg)	Water (kg)	Fine Sand (kg)	PP fibre (kg)	Foam (m ³)		Superplasticizer (kg)	
Sequence I	1	1500	580	—	580	348	—	—	—	0.2	9.2	1515
	2	1500	580	—	580	348	—	—	7.2	0.2	10.0	1528
	3	1300	507	—	507	304	—	—	—	0.3	8.0	1320
	4	1300	507	—	507	304	—	—	7.2	0.3	8.5	1326
	5	1000	435	—	435	130	—	—	—	0.4	6.9	1028
	6	1000	435	—	435	130	—	—	7.2	0.4	7.3	1033
	7	800	362	—	362	108	—	—	—	0.5	5.8	844
Sequence II	1	1500	493	87	580	348	—	—	—	0.2	11.6	1520
	2	1500	493	87	580	348	—	—	7.2	0.2	12.0	1530
	3	1300	431	76	507	304	—	—	—	0.3	10.1	1331
	4	1300	431	76	507	304	—	—	7.2	0.3	10.4	1338
	5	1000	359	65	435	130	—	—	—	0.4	8.7	1045
	6	1000	359	65	435	130	—	—	7.2	0.4	9.1	1050
Sequence III	1	1800	541	—	—	243	—	—	—	0.2	—	1846
	2	1800	541	—	—	243	1080	—	—	0.2	—	1833
	3	1800	370	65	435	243	620	—	—	0.2	—	1817
	4	1900	541	—	—	243	1080	—	—	0.2	—	1931
	5	1900	541	—	—	243	1080	—	—	0.2	—	1938
	6	1900	541	—	—	243	1080	—	—	0.2	—	1944

Fig. 2 Fresh density against target density

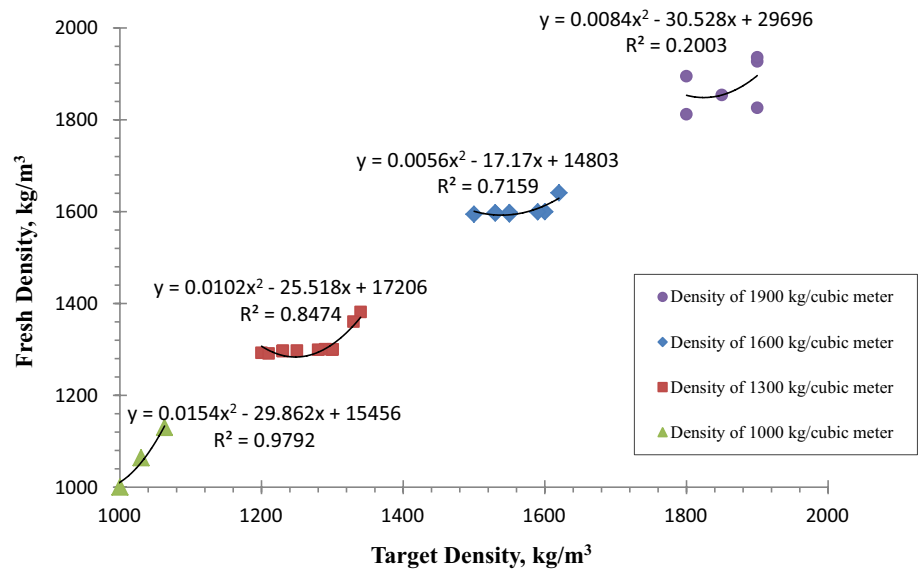
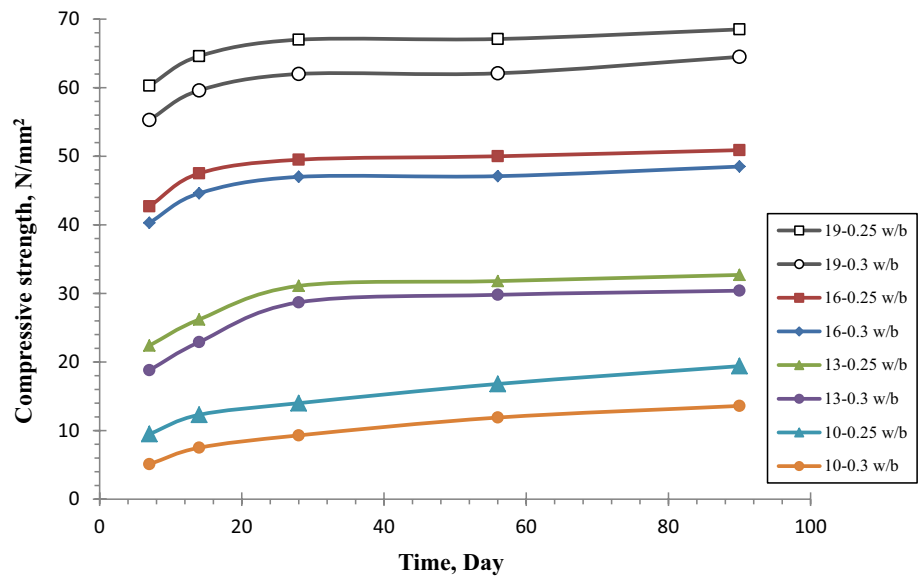


Fig. 3 Compressive strength against time for FC



Annotations: 19 = 1900 kg/m³, 16 = 1600 kg/m³, 13 = 1300 kg/m³, and 10 = 1000 kg/m³, and the (0.25, and 0.3) water/binder ratio.

lower than that reported by Pan et al. [38] but that produced the same density. Nonetheless, the strength of the former was still significantly greater than that of the conventional FC. Therefore, high-strength FC cannot be fabricated without adopting any ultrafine material with fineness higher than 7500 cm²/g, such as SF.

Density and foam volume

The relationship between the 28-day strengths of FC and the flow rate of the premixed paste is shown in Fig. 5. The hardened strength of FC significantly varied with the

disparity in the flow level of the premixed paste. Initially, the strength increased as the flow increased. After the peak was reached, the reverse phenomenon occurred in all of the FC with target densities of 1900, 1600, and 1300 kg/m³. An optimal point was visible in all of the curves. The peak strength was observed at flow values of 210–280 mm. The specimens with a target density of 1000 kg/m³, which were formed with 0.3 w/b ratio, initially showed an increasing trend of compressive strength with the flow. However, the apparent peak was observed at a flow value of approximately 280 mm, which was higher than the previously mentioned values. Accordingly, the voids in FC consisting of premixed

Fig. 4 Rate of development of strength at different ages for FC without SF

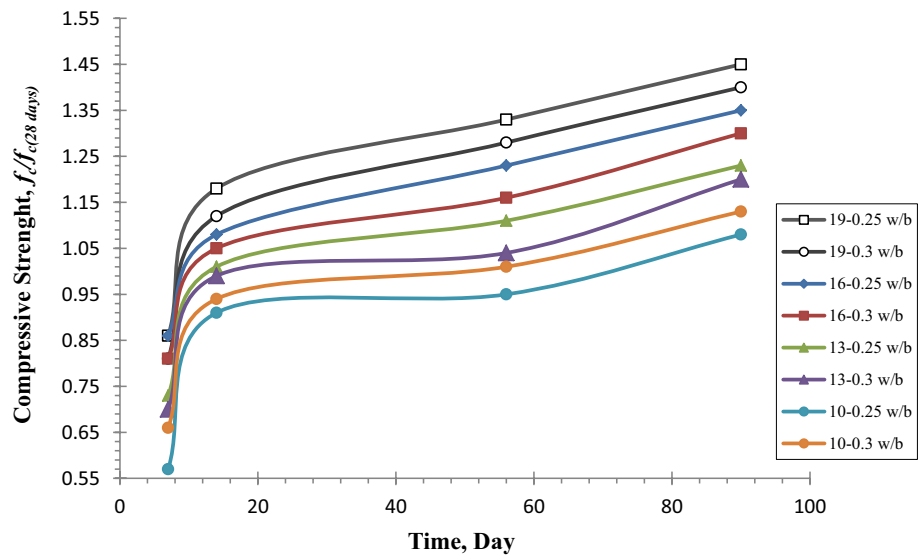
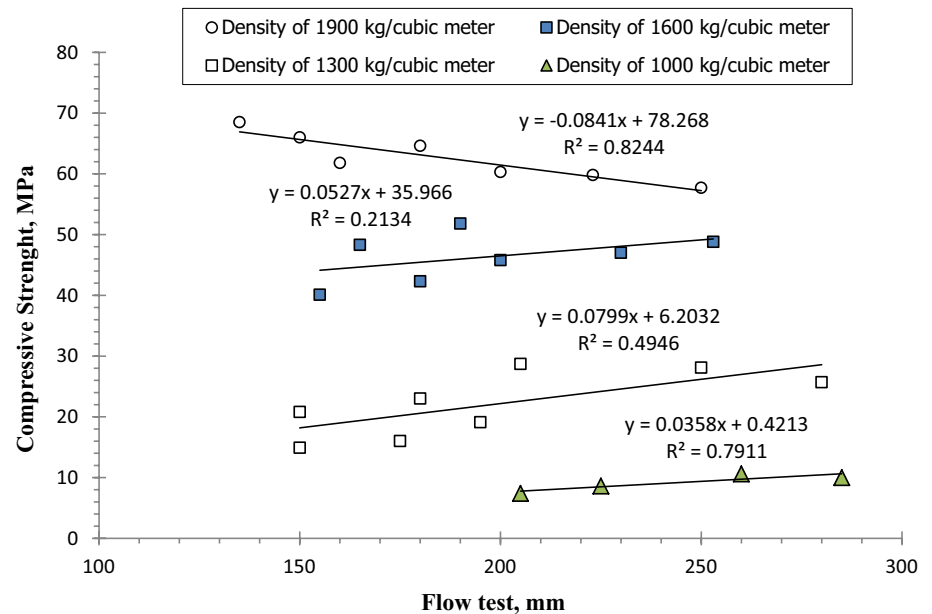


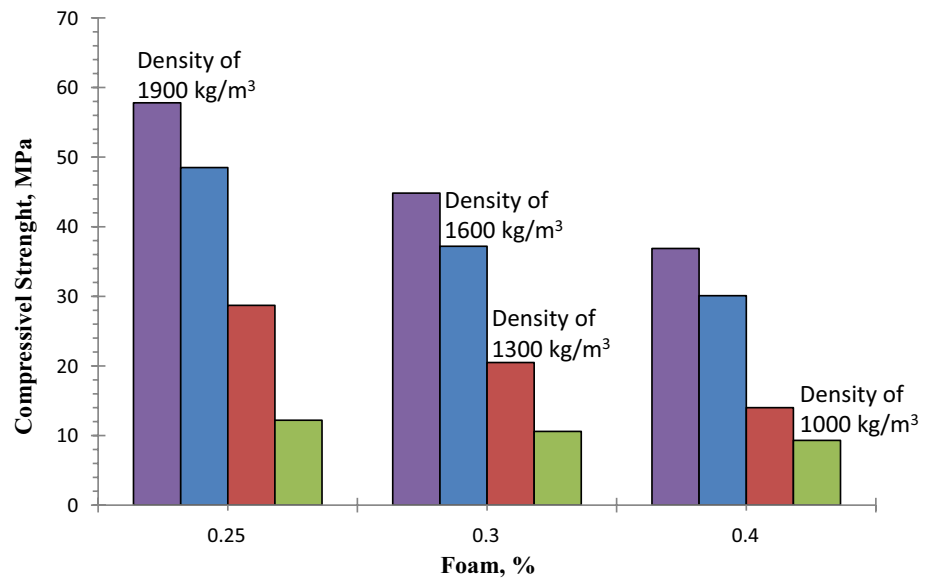
Fig. 5 Compressive strength against flow rate for FC



paste with a low value of flow appeared to be considerable. The dissimilarity in the distribution of pore size was another potential cause for the disparity in the hardened strength of the FC types. Another probable influencing parameter that affected the FC strength was the developed bond between the particles of cement content. The tide of the premixed paste represented the stress of shear within that paste. The improper and insufficient dispersion and the repulsion of cement particles within the mixture disrupted foaming action because the bridging of the foaming particles weakened the bonding between the cement particles. The FC strength increased rapidly with the density of concrete mass or with lessening foam volume (Fig. 6). Previous outcomes [39] indicated that this relationship remained linear within

the definite ranges of FC densities; however, in the wide possible ranges of densities, a curvilinear relationship was observed. As shown in Fig. 6, the slope of the strength–density curve increased with density but decreased with increasing foam volume. The slope was steeper in FC with SF than in FC without SF. In FC specimens without SF and with density of 1900 kg/m³, 58, 42, and 31 MPa of compressive strength was observed in the specimens with foam volumes of 20%, 30%, and 40%, respectively. Thus, the densities of these FC specimens were only 63%, 57%, and 47% of normal concrete, respectively. In FC specimens with SF, when the foam volume was 20%, 30%, and 40%, the strength reached 68.0, 39.5, and 24.8 MPa, correspondingly. Consequently, the lightweight FC material can develop strength equal to

Fig. 6 Compressive strength against percentage of foam agent added

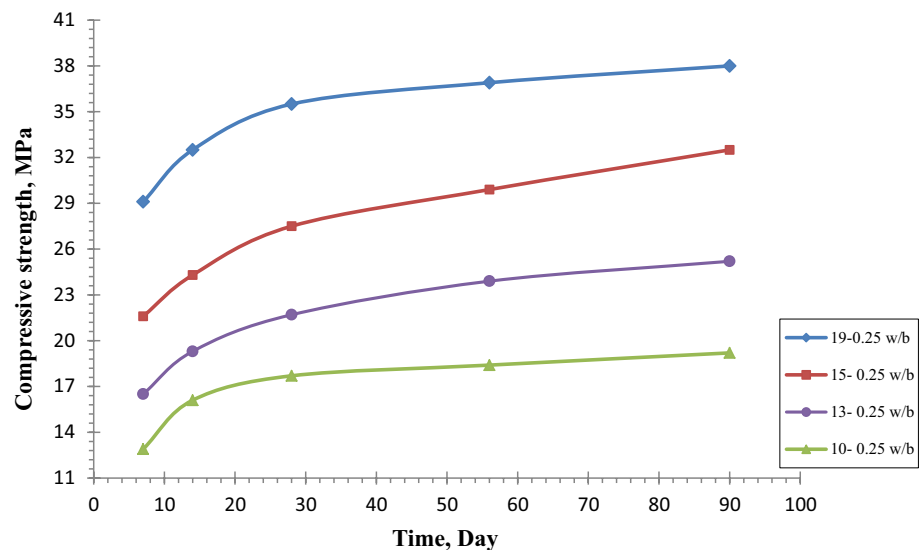


60 MPa with a density of approximately 60–70% of the traditional concrete density.

Silica fume

As shown in Fig. 7, with a similar foam volume, the addition of fine SF can considerably increase the hardened strength, up to 20–30% in most cases [40]. However, in FC with different foam volumes, the observed increment in strength varied. When the volume of foam was 25%, the strength was increased nearly by 21% (Fig. 6). When the volume of foam was approximately 40% (Fig. 6), the increase in compressive strength was around 30%. Therefore, with the addition of suitable foam content, SF can considerably improve the FC strength.

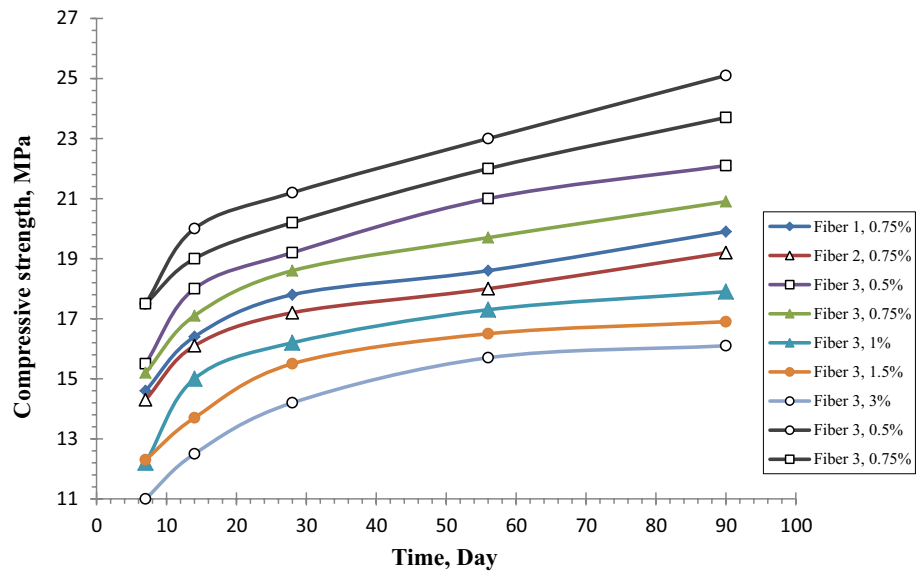
Fig. 7 Compressive strength against time for FC with SF



PP fibre

The influence of PP fibre on the hardened strength of the FC is depicted in Fig. 8. For a specified volume of foam, the PP fibre significantly improved the hardened strength. The variation in the increase rises with foam volume (Fig. 6). The compressive strengths of various curing ages for specified densities of 1900, 1500, 1300, and 1000 kg/m³ were 19%, 17%, 28%, and 39% higher than the reference, respectively. This advantage was also observed in the FC specimens with SF. Nevertheless, in all of the attempts, the addition of PP fibre condensed the flowability of the mix. Thus, we increased superplasticizer dosage to make the mixes flowable [1, 41, 42]. FC with high fibre content failed to progress because of poor workability; thus, the inclusion of 0.8% fibre content was the best adding level on the basis of a swap

Fig. 8 Compressive strength against time for FC with PP



between performance enhancement and flowability loss (Fig. 9) [1, 3]. FC with altered fibre volume fraction and different fibre types (Fig. 9) showed different rates of strength growth, possibly due to the modification in superplasticizer dosage. This modification may have delayed the hydration process, especially when the dosage was high [41].

Modulus of elasticity

A higher ratio of cylinder to cube strength was observed in cement paste and mortar because the absence of coarse aggregate resulted in good homogeneity [43]. Therefore, the sizes and shapes of the aggregates had a slight effect on the strength of the specimens. Although the FC was enclosed in merely fine aggregate, the air bubbles can be deemed as aggregates with zero elastic modulus and

strength. Three dissimilar kinds of fibres were included in this research. Figure 10 displays the influence of the volume of the foam agent on the hardened strength of the FC when a similar volume of foam (0.25–0.4%) was used in each mix. The FC with 0.25% volume of foam attained the peak FC compressive strength for all curing ages because the addition of 0.25% foam agent can develop a greater elastic modulus than the other additions. Furthermore, the specific gravity of type 3 fibres was more similar to the specific gravity of the FC than the other types. Such specific gravity is essential to the production of a uniformly distributed, homogeneous mixture. ACI 318 [40] provides the relationship between the elastic modulus in line with the measured strength and weight of concrete from experimental tests. The relationship was obtained by using Eq. (1) [40] (Fig. 11),

Fig. 9 Rate of development of strength at different age for FC with PP

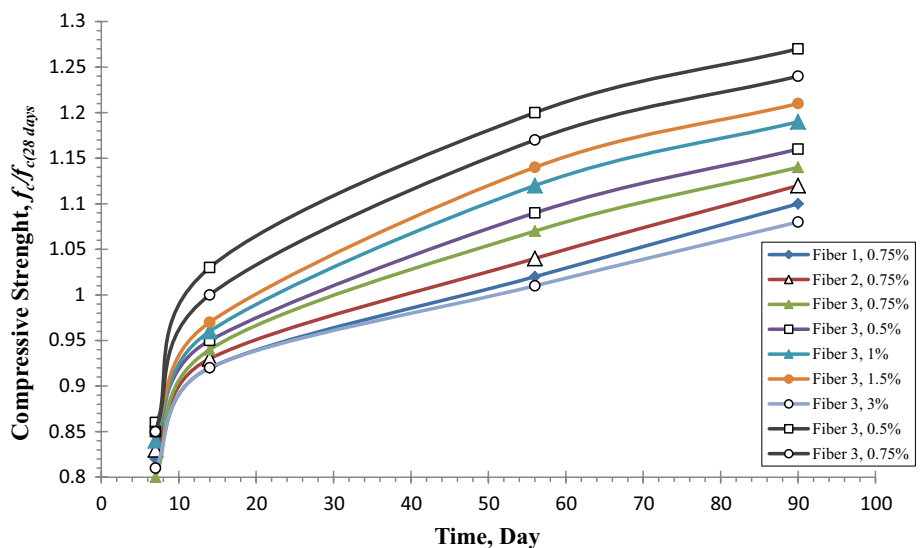


Fig. 10 Modulus of elasticity against percentage of foam agent added

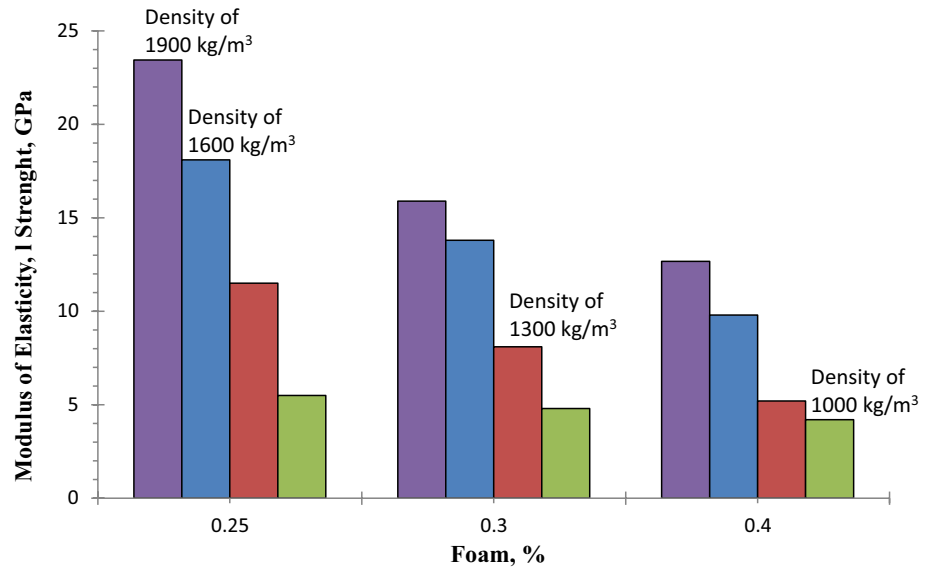
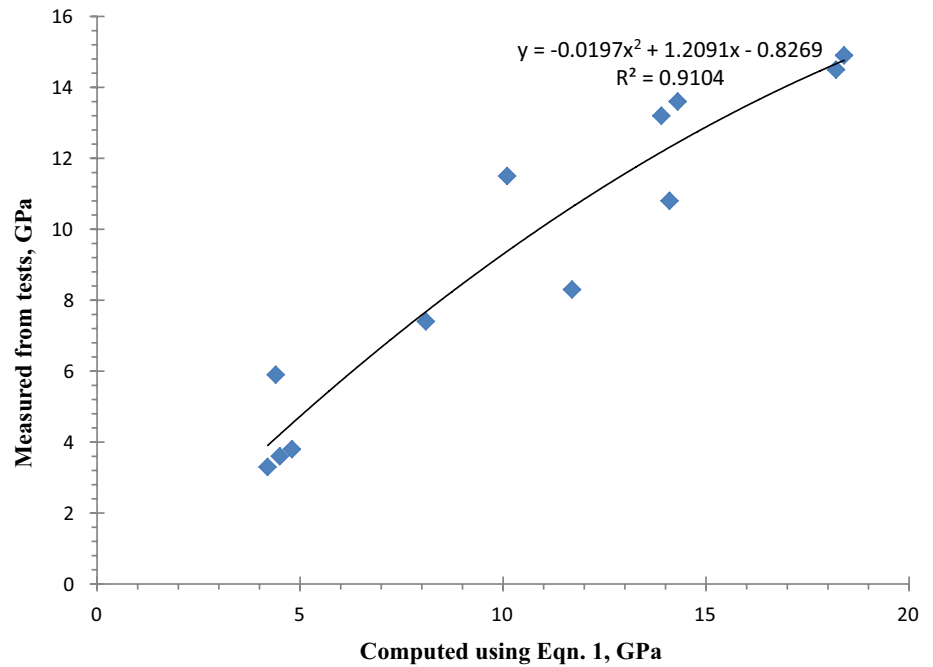


Fig. 11 Measured modulus of elasticity from tests against that computed using Eq. 1



$$E = W^{1.5} \times 33 \times \sqrt{f_c} \tag{1}$$

where the value of W (weight of concrete) ranges between 1440 and 2490 kg/m³.

Influential parameters of splitting tensile strength

Density and water-to-binder ratio

As observed in the results, tensile and compressive strengths of FC reduced with the increasing volume of foam content [1]. The disparity in tensile strength (f_t) and the variation in

compressive strength are revealed in Fig. 12. The FC with lesser w/b ratio and greater density attained greater tensile strength than the other FC specimens, although the compressive strength augmented with tensile strength.

Additionally, Fig. 13 shows the relationship between splitting tensile strength and w/b ratio in the four different densities. The ratio tended to be higher in FC with low density than in FC with high density and varied greatly in the former and slightly in the latter as the water-to-binder ratio increased [1, 3]. In FC without FA and SF, the average ratios were 0.0345, 0.0579, 0.0898, and 0.0939 for mixes with densities of 1900, 1600, 1300, and 1000 kg/m³, respectively.

Fig. 12 Splitting tensile strength with different densities

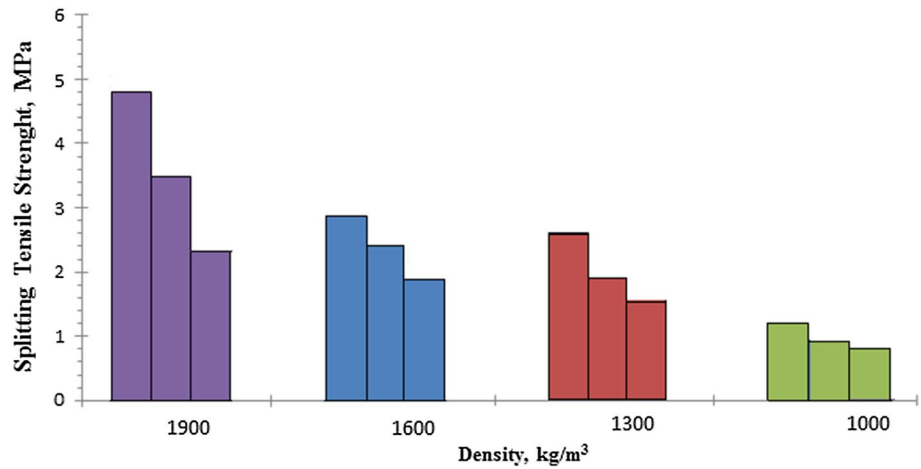
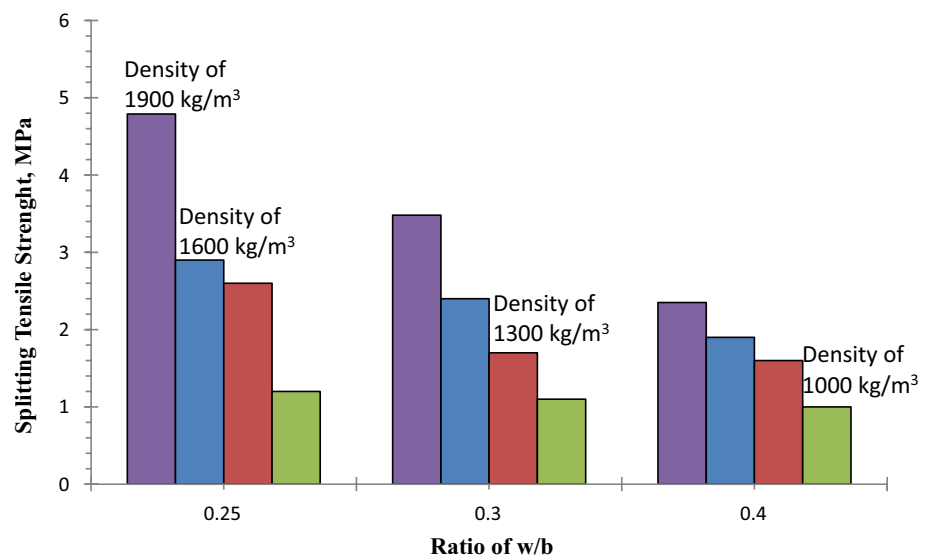


Fig. 13 Splitting tensile strength against percentage of foam agent added



PP fibre

Figure 14 shows the influence of PP fibre on the tensile strength of the FC with variable percentages of volume of foam in specimens. The inclusion of PP fibre prominently augmented the splitting tensile strength of FC [1, 3, 5]. However, the improvement in strength led to a sharp growth in foam volume. This result was indicative of the valuable influence of the addition of PP fibres. For the FC specimens with FA and SF combined with a 20% volume of foam, the tensile strength was observed 35.6% higher than that of FC deprived of PP fibre; meanwhile, for specimens with 25%, 35%, and 40% volumes of foam, the tensile strength augmented by 38%, 40%, and 45%, correspondingly. Similarly, this increment rate was likewise altered after the addition of SF in FC. In FC without FA and SF [44], the 28-day tensile strengths at 25%, 20%,

30%, and 40% volumes of foam were 36%, 31%, 38%, and 49% greater than the equivalent controls, correspondingly.

Influential parameters of flexural strength

Density and foam volume

The variations in the flexural strength of FC, at 28 days, with numerous w/b ratios and densities are shown in Fig. 15. The flexural strength of FC usually increases with density. Flexural strength had an opposite relationship with w/b ratio, except in the mix design with 1600 kg/m³ density and 0.2 w/b ratio because the flexural strength of this specimen was lower than the flexural strengths of the other specimens. This difference in flexural strength can be due to the high brittleness of hardened FC with a small w/b ratio [1–3]. The formation of a pocket due to

Fig. 14 Splitting tensile strength with different volumes of PP

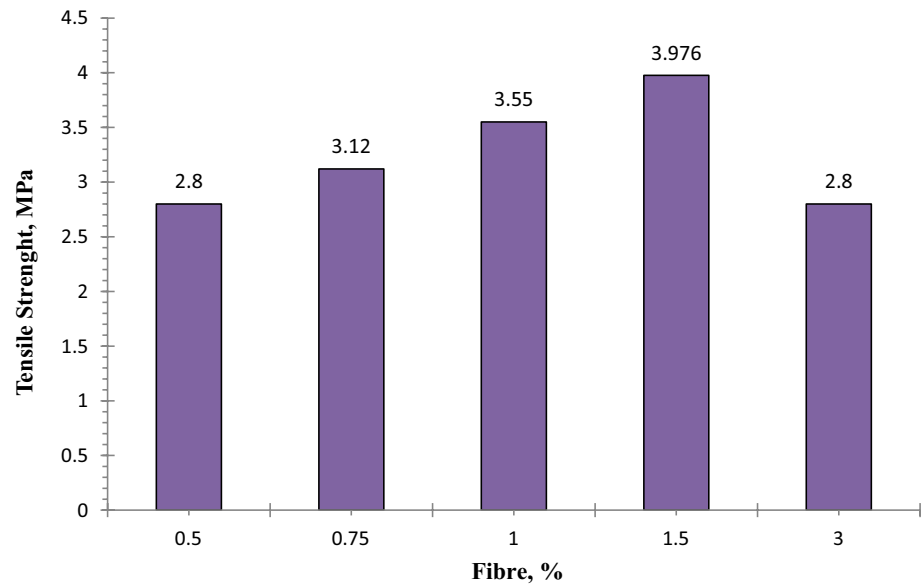
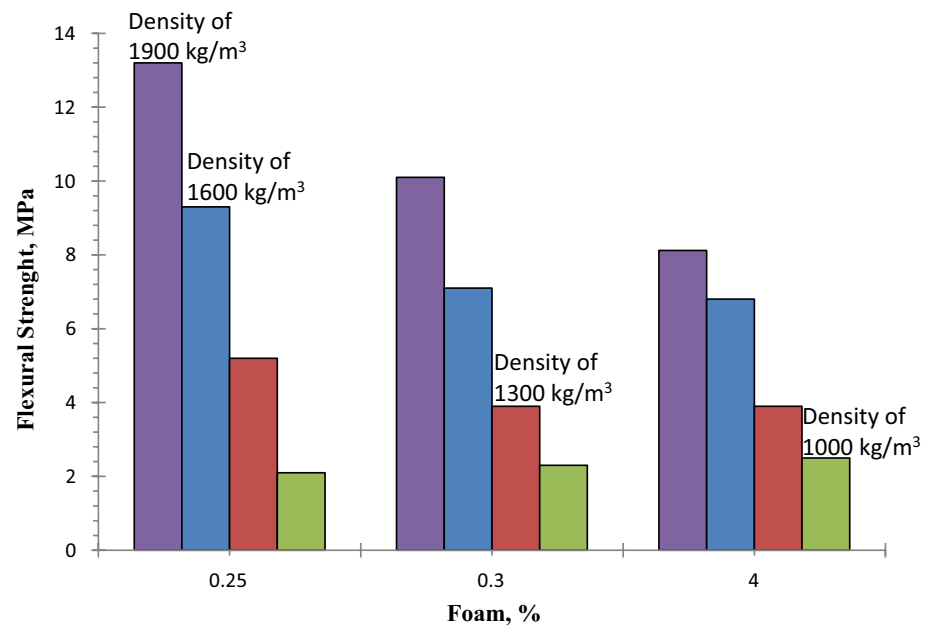


Fig. 15 Flexural strength against percentage of foam agent added

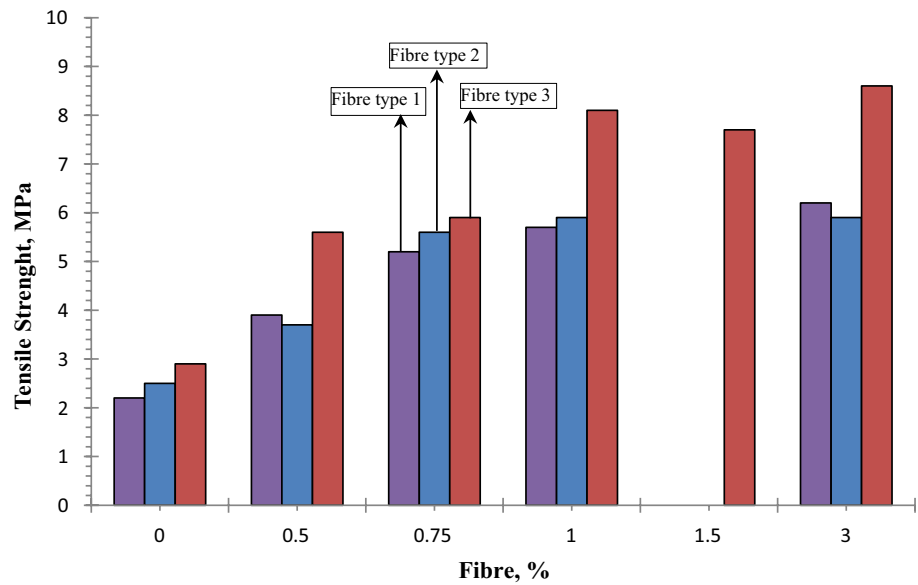


localized drying may account for the micro-crack development within FC. The pocket may be a result of incomplete hydration of cement paste and a resulting strength reduction. Several micro-cracks amalgamate readily at a low load level and result in low flexural strength. The rate of compressive strength to flexural strength generally increases with w/b ratio [1–3, 5–7, 19]. FC samples with a 0.25 w/b ratio and 1600 kg/m³ density displayed a greater ratio of compressive strength to flexural strength than the samples with densities of 1000 and 1300 kg/m³. Nonetheless, FC with low density and increased w/b ratio showed greater proportion of upsurge in the ratio of compressive strength to flexural strength than the other FC specimens.

Type of fibre

Three dissimilar kinds of PP fibres were utilized in the mix design of the specimens. The influence of the kind of PP fibres on flexural strength is depicted in Fig. 16. The addition of type 3 fibre augmented the flexural strength and the ratio of compressive strength to flexural strength to levels higher than those obtained by using the other fibre types. The ductility of hardened FC improved tremendously after the addition of type 3 fibre. The addition of the same volume of type 3 fibre (0.75%) resulted in a high flexural strength in each mix. Thus, the highest values of flexural strengths were obtained at all ages. Type 3 fibre had greater elastic modulus

Fig. 16 Flexural strength against type of PP fibres



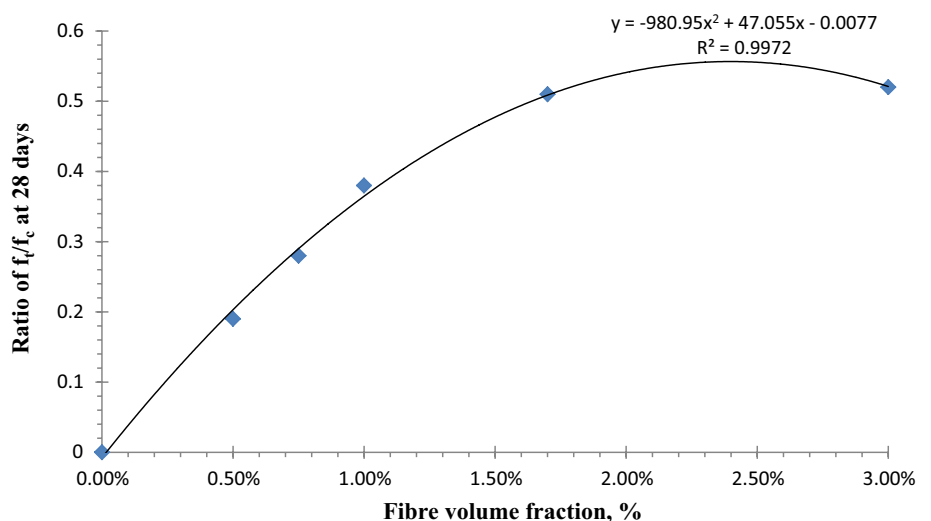
than the other types and hence strengthened the FC under bending action. Additionally, the specific gravity of type 3 fibre was nearly similar to that of the FC, unlike the other types. Thus, the mixture was homogeneous. Therefore, type 3 fibre more effectively increases the ductility of hardened FC than the other types.

Fibre volume fraction

Figure 17 explains the relationship of fibre volume fraction with the ratio of compressive strength to flexural strength. The fibre in FC effectively enhanced the flexural strength and the ratio of compressive strength to flexural strength [1,

3, 19, 44], which ranged from 0.19 to 0.52. For example, a 1.5% fibre volume fraction of type 3 fibre resulted in a lower strength than 1% volume fraction of a similar fibre. Nonetheless, the ratio of compressive strength to flexural strength was still high, and the mix became increasingly ductile. The performance of the mixes containing 0.75% and 1% type 3 fibre volume fractions was superior to that of the other mixtures. A 1% volume fraction of fibres appeared ideal, and content higher than this fraction might be excessive. For the addition of 0.5% volume fraction of fibre, no considerable influence was observed. Therefore, a range of volume fraction of fibre limited to between 0.75 and 1% was suitable for the effective development of FC.

Fig. 17 Rate of compressive strength to flexural strength against volume fraction of fibre at 28 days



Influential parameters of drying shrinkage

Age of drying

Figure 18 illustrates the difference in the shrinkage strain of FC with the ratio of foam volume, without addition of SF, to age. The samples at similar curing times showed an increasing trend in the shrinkage strain at increased foam volumes. When the volume of foam increased to around 55%, the strain of shrinkage was considerably greater than shrinkage strains of the other specimens at a similar curing time. This result of increasing trends was found to be parallel with the current practice of studies [46, 47]. The whole tested specimens deprived of PP fibre showed strain of drying shrinkage limited to between 400×10^6 and 1250×10^6 , which was detected beyond 150 days of curing in FC with

a 1000 or 1900 kg/m³ density. Moreover, the addition of SF slightly influenced the shrinkage.

PP fibre

Figure 19 demonstrates the impact of PP fibre on the FC shrinkage specimens with dissimilar volumes of foam at different curing periods. The inclusion of a large volume of PP fibres prominently decreased the drying shrinkage value [1, 3, 6, 7, 19, 46]. The drying shrinkage strain in all of the FC specimens with PP fibre was between 900×10^6 and 1300×10^6 at a curing time of 150 days. After the addition of type 3 fibre with 3% volume, the drying shrinkage values were much lower than those of the FC without fibres. Therefore, the inclusion of PP fibre in FC can increase the drying shrinkage characteristics of FC [46, 47].

Fig. 18 Strain of drying shrinkage against time

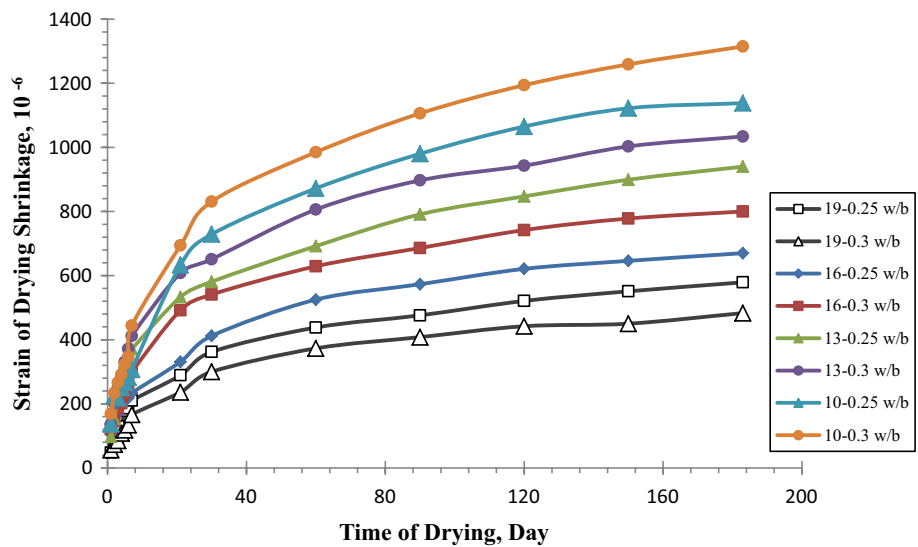
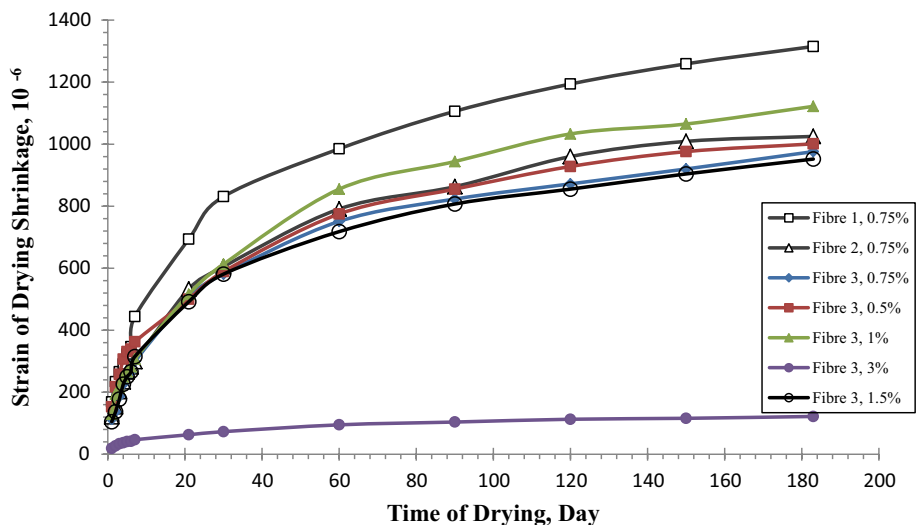


Fig. 19 Influence of volume and type of fibres on strain of drying shrinkage



Creep

According to the ASTM C 512 [36] standard, specimens shall be cured and stored under heat of 23 ± 2 °C. Nevertheless, the regular temperature in Malaysia was greater than standard. Consequently, 30 ± 2 °C was maintained for the curing and storage of the samples. Additionally, the standard recommended that the RH for storage samples is about $50 \pm 5\%$. The regular RH in Malaysia is greater than that limit value. Hence, the samples were stored at RH of $65 \pm 5\%$. The cylinder specimens ($\phi 150 \times 300$ mm) were moist cured at a heat of 30 ± 2 °C up to the seventh day. The samples were consequently placed in a creep chamber with a 30 ± 2 °C room temperature and $65 \pm 5\%$ RH. The samples were prepared for testing at 28 days. The strengths

of the samples were measured directly before the samples of creep were loaded in accordance with ASTM C 39 [45]. Around 20–25% stress of compressive strength was applied to the specimens. The reading on the strains was recorded before loading and immediately after loading on the first day (Figs. 20, 21). The creep strain was recorded on a daily basis in the first 1 week, then weekly for 1 month, and finally monthly up to the end of the half of a year [38, 40]. The deformation caused by the other factors rather than the loads was measured from unloaded specimens with the same curing and storage conditions. Strain of creep readings after half a year was not considered because of insufficient time. The rigs used for creep tests were a hydraulic type. Therefore, adjustment of loads could be done automatically after applying stress to the controller. Thus, it was not necessary

Fig. 20 Percentage of creep strain against time

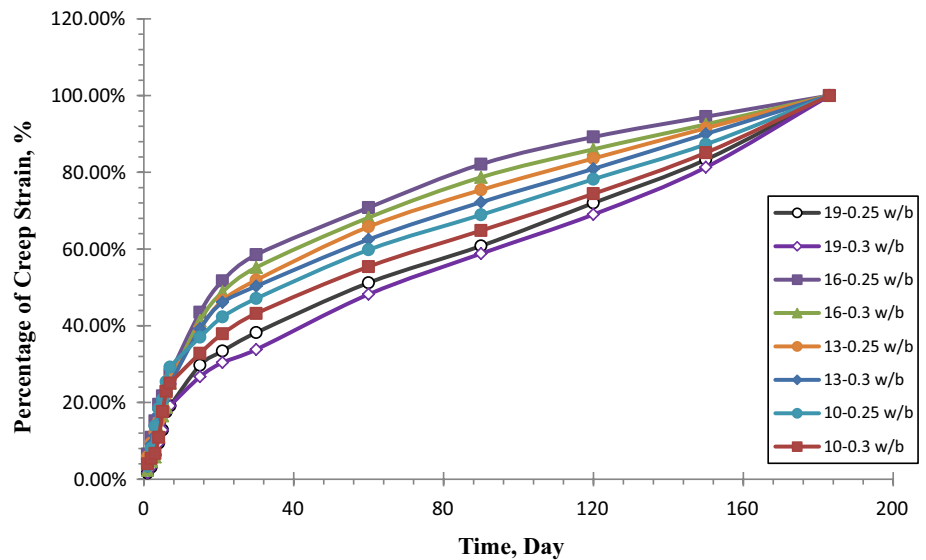
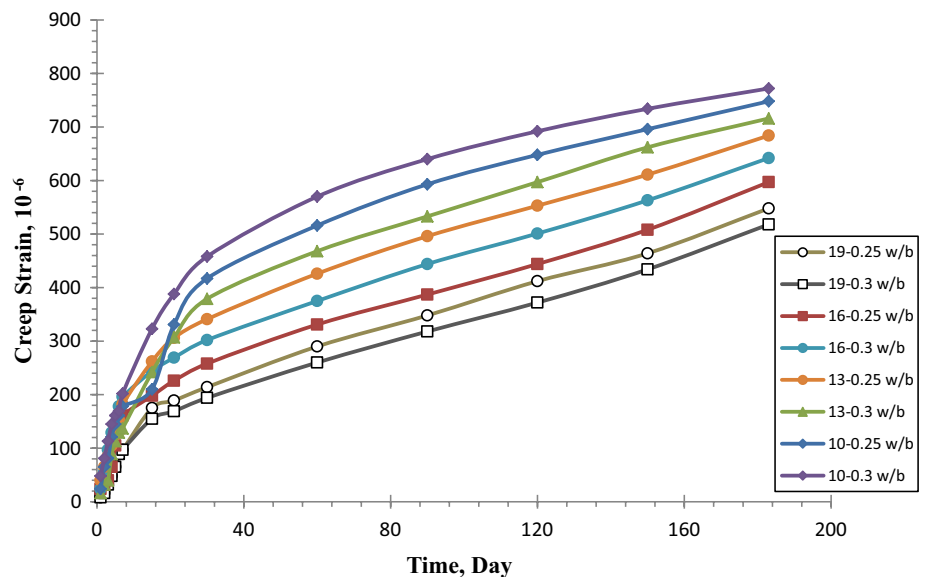


Fig. 21 Creep strain against time



to record the loads before the reading on each strain was obtained.

In accordance with the ASTM C 512 [36] standard, the elastic strain was measured and evaluated through experiments (Fig. 21). At 5 months, the resulting creep strain of FC was between 434 and 734×10^{-6} . Figures 20 and 21 present the ratio of creep strain at different ages to the average value of the ratio for all mixes at each age. Approximately, 50% of the total creep strain occurred at the first month of load application. However, no significant effect on water-to-binder ratio was observed on the creep of FC [1, 3, 5, 7, 46–48].

Thermal conductivity

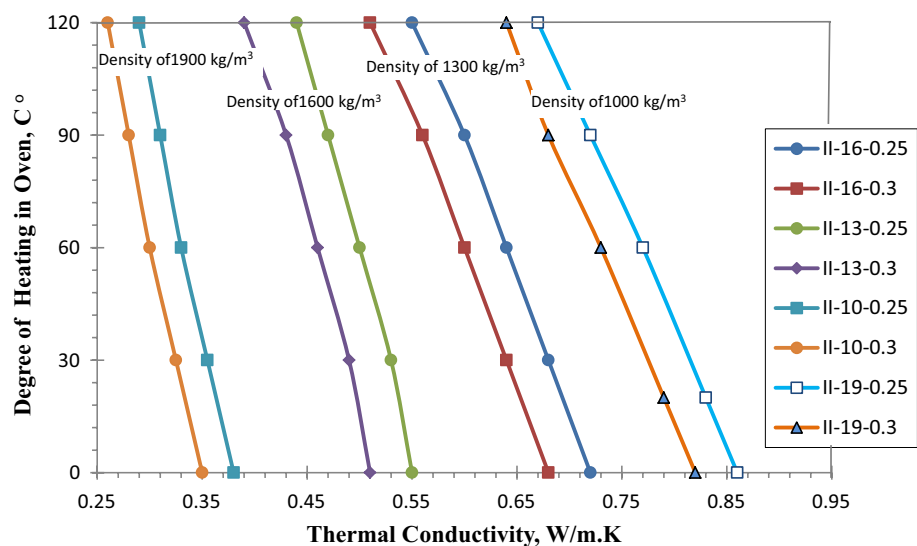
The thermal conductivity of FC was tested in line with the standards of ASTM C 177 [49]. Thermal conductivity of FC greatly depended on the thermal conductivity and relative proportion of each constituent. Air has much lower thermal conductivity than the other components, and the FC had a considerably high void content. Thermal conductivity was significantly affected by the volume of the voids [45, 50]. Additionally, the void content of FC varied with desired density. Therefore, the thermal conductivity of FC with dissimilar mixing proportions, but the same density, varied only slightly because the change in the distribution of pores was subtle. Some of the FC specimens were cured in moist condition until the 27th day and then oven-dehydrated at 30°C for a whole day. The temperature was maintained at 30°C for the measurement of thermal conductivity. The specimens were then oven-dried at temperatures up to 120°C , with 30°C as a constant increment, and consequently subjected to thermal conductivity tests at these temperatures (Fig. 22). At 120°C , the test of thermal conductivity involved cooling down the samples in a closed vessel and subjecting them

to 30°C , 60°C , and 90°C temperatures successively. The other specimens were subjected to moist curing until the 27th day and then oven-dried at 120°C for a whole day. Consequently, the test was performed at 120°C . Oven drying was performed for the eradication of the influence of moisture content on thermal conductivity [50]. Figure 22 shows a decreasing trend in the thermal conductivity of FC when heat was augmented from 30°C up to 120°C . Meanwhile, the specimens that were oven-dried at 120°C primarily and thereafter opened at a testing temperature that gradually reduced from 90 to 30°C showed increased thermal conductivity at augmented heat. The thermal conductivities were 0.56 and 0.64 W/m K at 1600 kg/m^3 FC density and 0.25 w/b ratio. Therefore, the thermal conductivity was affected by the moisture content and temperature of the FC. In the samples oven-dried at 120°C before the test, no change in weight was observed at low temperatures. Therefore, no remarkable change in the moisture of the specimens was found, and temperature is the key factor that controls the variation in thermal conductivity of FC [51].

Conclusions

This research paper presents structural fibred-foamed concrete made with FA, SF, and PP fibres for structural applications, evaluated in terms of specified parameters. A structural FC with a density of 1000 – 1900 kg/m^3 and correspondent compressive strength and splitting tensile strength of almost 10 – 70 MPa and 1.1 – 4.81 MPa, respectively, were developed by the inclusion of SF and PP fibres. The growth ratio of hardened strengths in FC to curing age increased with the inclusion of SF. For instance, the 28-day strength of FC with FA was around 80 – 95% of the corresponding strength observed after 3 months of curing. It is

Fig. 22 Degree of heating in oven against thermal conductivity



found that the strength of FC specimens with foam volumes of 20%, 30%, and 40% reached 68.0, 39.5, and 24.8 MPa, correspondingly. This demonstrated that the addition of suitable foam content with fine SF can produce strengths equal to 60 MPa with a density of approximately 60–70% of traditional concrete. At the specified volume of foam, the inclusion of PP fibre and SF enhanced the strengths of FC to levels 20–50% greater than those of the corresponding reference concrete.

Meanwhile, it is observed that FC with high fibre content failed to progress because of poor workability; thus, the inclusion of 0.8% fibre content was the best adding level on the basis of a swap between performance enhancement and flowability loss. Also, the FC with 0.25% volume of foam attained the peak FC compressive strength for all curing ages because the addition of 0.25% foam agent can develop a greater elastic modulus than the other additions. Likewise, an increment in the tensile strength was seen along with increased compressive strength. It is also found that the tensile strength of FC specimens with both FA and SF and a 20% volume of foam was observed to be 35.6% higher than that of FC deprived of PP fibre; meanwhile, for specimens with 25%, 35%, and 40% volumes of foam, it was augmented by 38%, 40%, and 45%, correspondingly.

This rate of increase was similarly altered with the addition of SF in FC. In FC without FA and SF, the 28-day tensile strengths at 25%, 20%, 30%, and 40% volumes of foam were 36%, 31%, 38%, and 49% greater than the equivalent controls, correspondingly. Completely, the FC exhibited the great drying shrinkage and creep results of $(900–1300) \times 10^6$ and $(434–734) \times 10^{-6}$ at 150 days, respectively. In similar mix proportions, the shrinkage increased with foam volume at the same curing age. The addition of SF had a slight influence on drying shrinkage. The same FC mix with PP fibre improved the shrinkage resistance property, where the values ranged from 900×10^6 to 1300×10^6 at 150 days. Furthermore, the thermal conductivity of FC reduced with an increase in oven-drying temperature from 30 to 120 °C. However, the improvement in hardened strength of FC led to a sharp growth in foam volume, observing that the FC was reducing with the increase in foam volume and can gain long-term strength. This result was indicative of the valuable influence of the addition of PP fibres with a suitable range of volume fraction limited between 0.75% and 1% for the effective development of FC. Therefore, structural fibred-foamed concrete (SFFC) is a prospective, lightweight concrete product that can possibly be utilized as an alternative material for structural concrete applications in the construction industries today.

Acknowledgements The authors gratefully acknowledge the financial support by the Department of Civil Engineering, College of Engineering, Prince Sattam Bin Abdulaziz University, Saudi Arabia; and

the Department of Civil Engineering, Faculty of Engineering and IT, Amran University, Yemen (GRA201931), for this research.

Compliance with ethical standards

Conflict of interest The authors have no conflicts of interest to disclose.

References

- Amran YM, Farzadnia N, Ali AA (2015) Properties and applications of foamed concrete; a review. *Constr Build Mater* 101:990–1005
- Nambiar EK, Ramamurthy K (2007) Air-void characterisation of foam concrete. *Cem Concr Res* 37(2):221–230
- Ramamurthy K, Nambiar EK, Ranjani GIS (2009) A classification of studies on properties of foam concrete. *Cement Concr Compos* 31(6):388–396
- Just A, Middendorf B (2009) Microstructure of high-strength foam concrete. *Mater Charact* 60(7):741–748
- Jones M, McCarthy A (2005) Preliminary views on the potential of foamed concrete as a structural material. *Magazine of concrete research* 57(1):21–31
- Cox L, van Dijk S (2002) Foam concrete: a different kind of mix. *Concrete* 36:2
- Kearsley E, Wainwright P (2001) The effect of high fly ash content on the compressive strength of foamed concrete. *Cem Concr Res* 31(1):105–112
- Narayanan N, Ramamurthy K (2000) Structure and properties of aerated concrete: a review. *Cement Concr Compos* 22(5):321–329
- Karl S, Wörner J (1993) Foamed concrete-mixing and workability. In: *Special concrete-workability and mixing*. E & FN Spon London, pp 217–224
- Kearsley E, Wainwright P (2001) Porosity and permeability of foamed concrete. *Cem Concr Res* 31(5):805–812
- Amran YM, Ali AA, Rashid RS, Hejazi F, Safiee NA (2016) Structural behavior of axially loaded precast foamed concrete sandwich panels. *Constr Build Mater* 107:307–320
- Amran YM, Rashid RS, Hejazi F, Safiee NA, Ali AA (2016) Response of precast foamed concrete sandwich panels to flexural loading. *J Build Eng* 7:143–158
- Amran YM, Rashid RS, Hejazi F, Safiee NA, Ali AA (2016) Structural behavior of laterally loaded precast foamed concrete sandwich panel. *Int J Civil Environ Struct Constr Archit Eng* 10:3
- Singh D, Kumar A (2019) Mechanical characteristics of municipal solid waste incineration bottom ash treated with cement and fiber. *Innov Infrastruct Solut* 4(1):61
- Yip CC, Marsono AK, Wong JY, Amran MY, UTM Johor Bahru (2015) Flexural strength of special reinforced lightweight concrete beam for Industrialised Building System (IBS). *Jurnal Teknologi* 77(1):187–196
- Amran YM, Rashid RS, Hejazi F, Safiee NA, Ali AA (2016) Structural behavior of precast foamed concrete sandwich panel subjected to vertical in-plane shear loading. *World Acad Sci Eng Technol Int J Civil Environ Struct Constr Archit Eng* 10(6):705–714
- Dunton HR, Rez DH (1988) Apparatus and method to produce foam, and foamed concrete. U.S. Patent 4,789,244
- Hashimoto A, Hayashi S, Yamamoto S, Chujo H (1977) Misawa Homes Institute of Research, Development Co Ltd and Showa Denko KK. Process of continuous manufacture of light-weight foamed concrete. U.S. Patent 4,057,608

19. Bing C, Zhen W, Ning L (2011) Experimental research on properties of high-strength foamed concrete. *J Mater Civ Eng* 24(1):113–118
20. Hetzroni O, Harris O (1996) Cultural aspects in the development of AAC users. *Augment Altern Commun* 12(1):52–58
21. Amran YHM (2016) Determination of structural behavior of precast foamed concrete sandwich panel. Ph.D thesis, Universiti Putra Malaysia (UPM), p 345
22. Zhang Z, Provis JL, Reid A, Wang H (2014) Geopolymer foam concrete: an emerging material for sustainable construction. *Constr Build Mater* 56:113–127
23. Siddika A, Al Mamun MA, Ali MH (2018) Study on concrete with rice husk ash. *Innov Infrastruct Solut* 3(1):18
24. Pigeon M, Plante P, Plante M (1989) Air void stability, part I: influence of silica fume and other parameters. *Mater J* 86(5):482–490
25. Geetha S, Ramamurthy K (2013) Properties of geopolymerised low-calcium bottom ash aggregate cured at ambient temperature. *Cement Concr Comput* 43:20–30
26. Chatterji J, King BJ, Zamora F, Anderson CR, Bennett BJ, Cromwell RS (2002) High strength foamed well cement compositions and methods. U.S. Patent 6,500,252
27. Brothers LE, Turkett SM, Ekstrand BB, Brenneis DC, Childs JD (2002) Halliburton Energy Services Inc. Light weight high temperature well cement compositions and methods. U.S. Patent 6,488,763
28. Fernandes PA, Veludo J, Almeida N, Baptista J, Rodrigues H (2018) Study of a self-compacting fiber-reinforced concrete to be applied in the precast industry. *Innov Infrastruct Solut* 3(1):28
29. Bawa S, Singh SP (2019) Fatigue performance of self-compacting concrete containing hybrid steel–polypropylene fibres. *Innov Infrastruct Solut* 4(1):57
30. Meddah A, Merzoug K (2017) Feasibility of using rubber waste fibers as reinforcements for sandy soils. *Innov Infrastruct Solut* 2(1):5
31. ASTM C 618 (2003) Standard specification for coal fly and raw or calcined natural pozzolan for use as a mineral admixture in concrete. ASTM International, West Conshohocken
32. ASTM, C 469 (2002) Standard test method for static modulus of elasticity and Poisson's ratio of concrete in compression, vol 4. Annual book of ASTM standards, West Conshohocken
33. ASTM C 490 (2011) Standard practice for use of apparatus for the determination of length change of hardened cement paste, mortar, and concrete. ASTM International, West Conshohocken
34. Tattersall GH, Banfill PF (1983) The rheology of fresh concrete, Accession no.: 00385513. Transport Research Laboratory, 356 p
35. Powers TC (1968) The properties of fresh concrete. Wiley, New York, 301 p
36. ASTM C 512 (2010) Test method for creep of concrete in compression. ASTM International, West Conshohocken
37. Kearsley E, Visagie M (1999) Micro-properties of foamed concrete Specialist techniques and materials for construction. Thomas Telford, London, pp 173–184
38. Pan Z, Hiromi F, Wee T (2007) Preparation of high performance foamed concrete from cement, sand and mineral admixtures. *J Wuhan Univ Technol Mater Sci Ed* 22(2):295–298
39. Hoff GC (1972) Porosity-strength considerations for cellular concrete. *Cem Concr Res* 2(1):91–100
40. ACI Committee 318 (2005) Building code requirements for structural concrete and commentary. American Concrete Institute, West Conshohocken
41. Kunhanandan Nambiar EK, Ramamurthy K (2008) Fresh state characteristics of foam concrete. *J Mater Civ Eng* 20(2):111–117
42. Zhang P, Li QF (2013) Effect of polypropylene fiber on durability of concrete composite containing fly ash and silica fume. *Compos B Eng* 45(1):1587–1594
43. Neville AM (1995) Properties of concrete, vol 4. Longman, London
44. Priyadarshini M, Patnaik M, Giri JP (2018) A probabilistic approach for identification of compressive strength of fly ash bricks. *Innov Infrastruct Solut* 3(1):56
45. ASTM C 39 (2005) Standard test method for compressive strength of cylindrical concrete specimens. ASTM International, West Conshohocken
46. Awang H, Mydin MA, Roslan AF (2012) Effect of additives on mechanical and thermal properties of lightweight foamed concrete. *Adv Appl Sci Res* 3(5):3326–3338
47. Short A, Kinniburgh W (1963) Lightweight concrete. CR books, New York
48. Chindaprasirt P, Rattanasak U (2011) Shrinkage behavior of structural foam lightweight concrete containing glycol compounds and fly ash. *Mater Des* 32(2):723–727
49. ASTM C 177 (2004) Methods of measuring thermal conductivity, absolute and reference method. ASTM International, West Conshohocken
50. Wong Kit H (2007) Thermal Conductivity of foamed concrete. Ph.D. thesis, National University of Singapore
51. Liu MYJ, Alengaram UJ, Jumaat MZ, Mo KH (2014) Evaluation of thermal conductivity, mechanical and transport properties of lightweight aggregate foamed geopolymer concrete. *Energy Build* 72:238–245